6th International Conference on Advances in Experimental Structural Engineering
11th International Workshop on Advanced Smart Materials and Smart Structures Technology
August 1-2, 2015, University of Illinois, Urbana-Champaign, United States

Use of a Novel Distributed Fiber Optic Strain Measurement System in the Seismic Retrofit of RC Shear Walls

J. Woods[1], D. Lau[2], X. Bao[3], and W. Li[4]

1 Graduate Student, Dept. of Civil and Environmental Engineering, Carleton University, Ottawa, Canada. E-mail: josh.woods@carleton.ca
2 Professor, Dept. of Civil and Environmental Engineering, Carleton University, Ottawa, Canada. E-mail: david.lau@carleton.ca
3 Professor, Dept. of Physics, University of Ottawa, Ottawa, Canada. E-mail: xbao@science.uOttawa.ca
4 Post-Doctoral Fellow, Dept. of Physics, University of Ottawa, Ottawa, Canada. E-mail: Wenhai.Li@uottawa.ca

ABSTRACT:
This paper presents results on the application of a truly distributed fiber optic sensor (DFOS) in place of conventional strain gauges in experimental testing of a reinforced concrete (RC) shear wall retrofitted with fiber-reinforced polymer (FRP) sheets. The conventional strain measurement technique using electrical strain gauges requires a-priori knowledge of measurement location and does not provide spatial information over a large area of a structural component, such as a wall. In recent years, the development of novel fiber-optic sensing technologies offers clear advantages compared to the conventional strain measurement approach. In particular, the DFOS system has the unique capability of capturing strain at any location along the fiber without pre-determining the measurement locations before the test. The DFOS system allows full 2D spatial strain measurement over the entire area of a shear wall. The DFOS system can capture detailed response and failure mechanisms of the concrete and FRP as well as their contributions to the seismic resistance of the shear wall. Experimental results are utilized to develop a better understanding of the behavior of RC shear walls retrofitted with FRP sheets, and assist in improving design methodology and guidelines for the use of FRP in seismic repair and strengthening applications.

KEYWORDS: *distributed fiber-optic sensors, reinforced concrete, shear wall, FRP, seismic retrofit*

1. INTRODUCTION

Over the last several decades, there has been a significant amount of interest and research into the use of fiber-optic sensors for the measurement of strain and temperature. A number of different fiber-optic sensing techniques have been developed based on the intrinsic backscattering of fibers. In civil engineering applications, fiber-sensors have been shown to be capable of measuring strains, pressures, accelerations, and temperatures with a high degree of accuracy [1]. Although conventional mechanical and/or electrical transducers are able to measure the majority of these quantities, fiber-optic sensors can provide better quality measurements with a higher level of reliability, and easier installation. They are also more durable, stable, and insensitive to external perturbation. The use of distributed fiber-optic systems also has the added capability of being able to measure at many intervals over the entire length of a single fiber. As an alternative to conventional electrical strain gauges, or other fiber-optic systems such as the traditional Bragg grating system that require a priori knowledge of specific measurement locations, there are many benefits and applications for a truly distributed fiber-optic sensing system. In this study, the distributed fiber-optic sensor is implemented in an experimental program on the seismic retrofit of reinforced concrete (RC) shear walls retrofitted with externally bonded fiber-reinforced polymer (FRP) sheets. A RC shear wall strengthened using externally bonded FRP sheets is tested under simulated earthquake loads by applying quasi-static reversed cyclic load to the top of the wall. The goal of strengthening the wall using FRP is to increase the lateral load carrying capacity, ductility, and energy dissipation capacity of the wall specimen, and improve its seismic performance. Using the conventional strain measurement approach, the amount of data researchers are able to collect on the strain distribution in the FRP sheet has been limited by the number of sensors available and the size of the data acquisition system. However, using the DFOS system allows for a full high-resolution two-dimensional contour of the spatial strain distribution in the FRP. This information is utilized to perform a detailed analysis of the behavior of the FRP strengthening system at various stages throughout the test (ie. cracking, yield, and post-yield behaviour). In addition, results from the strain distribution are compared with maximum strain values used in design to improve design standards and the methodologies used in designing RC shear walls with externally bonded FRP sheets for improved seismic performance.

2. DISTRIBUTED FIBER OPTIC SYSTEMS

Several DFOS techniques have been developed based on the measurement of intrinsic backscatter, or the reflection of waves in small glass fibers. These techniques include Raman, Brillouin and Rayleigh scattering as well as those involving low-coherence reflectometry (OLCR) and frequency domain reflectometry (OFDR). Techniques based on Raman and Brillouin scatter measurement use optical time domain reflectometry (OTDR), which maps a specific position to the time of flight for a pulse to travel to and from the sensing location. OTDR technology has found applications for long distance distributed measurement, however, its measurement resolution is typically in the order of a meter, and is thus not well suited for applications that require high resolution measurement. Alternatively, OLCR uses low-coherence detection techniques to achieve very high spatial resolution (micrometer), but its measurement range is only in the order of several meters. This leaves the OFDR technique, which fills the gap between the OTDR and OLCR techniques and allows for resolution within the millimeter range over tens of to hundreds of meters [2], presenting an attractive solution for temperature and strain monitoring in civil engineering applications.

However, to discriminate between temperature and strain with a higher spatial resolution, high sensitivity is a necessary requirement for the success of any distributed sensing instrumentation project. A number of temperature and strain discrimination techniques have been proposed including methods that examine Brillouin gain amplitudes, Brillouin frequency shifts, and hybrid Raman-Brillouin gains [3-5]. These methods typically have a spatial resolution in the order of meters. This is different from a quasi-distributed sensing technique, such as using fiber Bragg grating, which is capable of higher resolution (within the centimeter order), and is able to distinguish between temperature and strain using a dual interrogation technique [6]. However, although fiber Bragg gratings can offer high-resolution strain and temperature measurement, they are often limited by the number of gratings available for a single fiber, thus reducing the practicality of the sensor when compared with conventional mechanical or electrical measurement techniques.

Recently, the OFDR technique has been shown to be able to discriminate between temperature and strain by using a polarization maintaining fiber (PMF) as the sensing fiber. In this approach, every resolved segment along the PMF is treated as a dual wavelength fiber Bragg grating pair [2], and the applied temperature and strain can be effectively separated through analysis of the spectra shifting of the segment. The advantage of this approach is that a single PMF effectively replaces a huge number of fiber Bragg gratings to make a truly distributed measurement technique. The measurement technique is capable of distinguishing between strain and temperature to within 1μ-strain and 0.1ºC with a 2.5mm spatial resolution over 180 meters of fiber [2]. This OFDR sensor system is adopted for the current experimental program and is the first of its kind to be used in RC shear wall monitoring with high strain and spatial resolution.

3. SHEAR WALL PROJECT

3.1 Methodology

To validate the performance of the DFOS in a civil engineering laboratory experiment, the DFOS is used as a replacement for conventional electrical gauges for strain measurement in an experimental study of the strain distribution and performance of FRP in the seismic retrofit of a RC shear wall. Reinforced concrete shear walls are common lateral load resisting systems used to resist forces induced on a structure from wind and earthquake loads. In this study, a series of RC shear walls designed using older design standards [7, 8] are tested under simulated earthquake loads. Because the walls are designed using older less-stringent design standards, there are a number of deficiencies in their design commonly found in many existing RC structures constructed during the 1960's and 1970's. The deficiencies in their design include insufficient shear reinforcement, poor confinement of the boundary elements, and a lower concrete compressive strength. These deficiencies lead to poor seismic performance, which is characterized by low lateral strength and a lack of ductility and energy dissipation capacity. To improve the seismic performance of a deficient RC shear wall, there are a number of retrofitting alternatives available. One innovative retrofitting solution is a system consisting of externally bonded FRP sheets. Previous studies have demonstrated the ability of using FRP sheets to improve the flexural and shear strength of RC shear walls designed according to modern design standards [9]. However, investigation into the shear and flexural strengthening of walls with poor seismic details has been limited. Fig. 3.1 shows the steel reinforcement and FRP detailing for a typical shear wall test specimen in this study. The wall is detailed with vertical and horizontal steel reinforcement ratios of 3% and 0.25% respectively. The lack of adequate horizontal reinforcement in these wall specimens has been shown to lead to sudden and brittle diagonal tension shear failure [10]. To improve the shear and flexural strength of the RC shear wall, FRP sheets are applied in the horizontal and vertical directions. A single vertical FRP sheet, and three horizontal FRP sheets are applied to each side of the wall. The vertical sheets improve the walls flexural capacity, something that may be required to meet modern seismic design standards. To ensure the wall specimen fails in a ductile manner, it is necessary to ensure the capacity against diagonal tension shear failure is higher than its flexural capacity. Three horizontal FRP sheets are required on each side of the wall to ensure the wall has sufficient shear capacity against diagonal tension failure. The shift from a brittle shear failure to a flexural mode of failure leads to better seismic performance including an increase in strength, ductility and energy dissipation capacity. Table 3.1 shows the material properties for the concrete, steel, and FRP reinforcement.

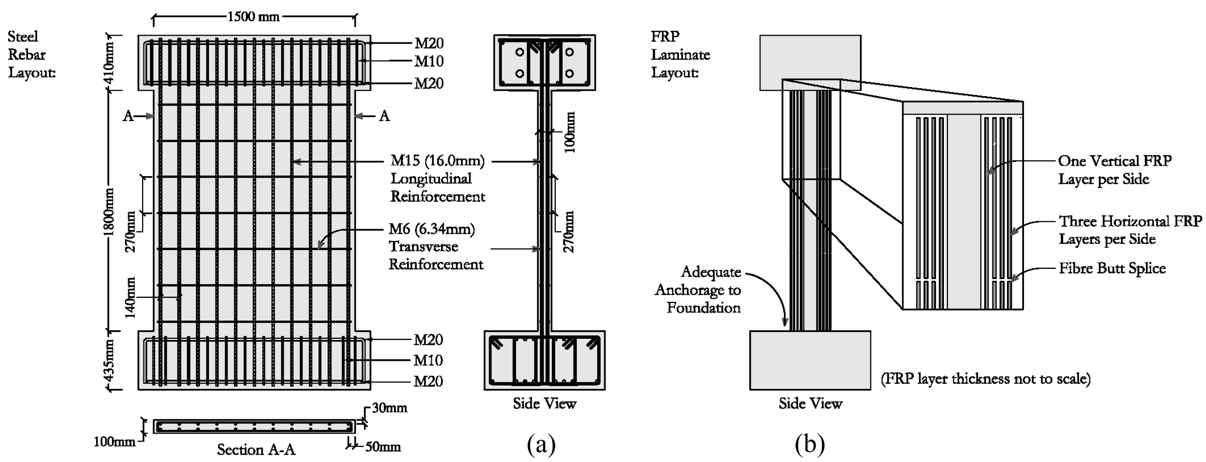

Figure 3.1 (a) Shear wall steel reinforcing details; (b) FRP reinforcement details

Table 3.1 Concrete, steel and FRP material properties

Concrete		Steel Reinforcement		FRP (Tyfo SCH-41)	
f_c'	19.1 MPa	f_y	439 MPa	f_f	834 MPa
ε_u'	0.0042	ε_y	0.002	ε_u	0.01
E_c	19.2 GPa	E_s	201 GPa	E_f	82 GPa

where f_c' is the concrete compressive strength; ε_u' is the ultimate compressive strain; E_c is the modulus of elasticity; f_y is the yield stress of the steel; ε_y is the yield strain; E_s is the Young's modulus; f_f is the ultimate tensile strength of the FRP section (fiber + epoxy); ε_u is the ultimate tensile strain (fracture strain); and E_f is the tensile modulus.

3.2 Test Setup and Instrumentation

To simulate the lateral drift demand and damage to a RC shear wall during a major seismic event, the wall specimen is tested under a predetermined reversed cyclic lateral load sequence. The wall specimen is fixed to the laboratory strong floor and a hydraulic actuator applies the lateral load to the top of the wall specimen. Two one-way hinges allow free rotation of the top of the wall, such that it acts as a cantilevered wall. Out-of-plane deformations of the wall are limited through the use of a lateral restraint frame. Fig. 3.2 shows a typical test setup. The specimen is first tested in load control, by applying lateral load up to 25%, 50%, 75% and 100% of the yield load. Two successive cycles are applied at each load level to observe any softening effects on the response of the wall. After reaching the yield load, the test is continued in displacement control by increasing the target displacement levels up to failure.

To measure the strain distribution over the entire face of the RC shear wall, the optical fiber is surface bonded to the FRP using an epoxy resin. The application of the fiber on the surface of the FRP is much less intensive when compared to the application of conventional electrical strain gauges, which require significant surface preparation prior to installation. The OFDR sensor system described in section 2 measures strain along its longitudinal axis, and it is assumed that the effects of strain in the transverse direction on the sensors output are minimal. Studies have demonstrated that by using epoxy to bond the fiber to the surface of the structural element, the strain transfer to the fiber in the transverse direction is poor because of the relatively low stiffness of the epoxy in comparison with the fiber [11]. In some cases, it may be more practical to embed the fiber into the FRP laminate during the FRP installation process. In doing so, the hardened FRP provides protection for the fiber-optic cable and provides a convenient means for the implementation of the optical fibers in RC structures [11]. However, because protection of the fiber is not as critical in a controlled laboratory environment, the fiber is surface bonded on top of the FRP after it is cured. As shown in Fig. 3.2, the fiber is first installed on the front side of the wall in the horizontal direction and then continues to the back of the wall where it is applied in the vertical direction. The fiber is oriented in separate horizontal and vertical directions on opposite sides of the wall to avoid interference between vertical and horizontal strain measurement. Because the out-of-plane displacement of the wall is being restrained, the strain on the front and back sides of the wall specimen is assumed to be approximately equal. In total, a single 50m long fiber is placed over the front and back surfaces of the wall. The OFDR sensor is capable of measuring strain accurate to within 1μ-strain at intervals of 10mm along the length of the fibre using standard communication fiber. Strain measurements from the OFDR are taken at the end of each load step, prior to alternating the direction of the load.

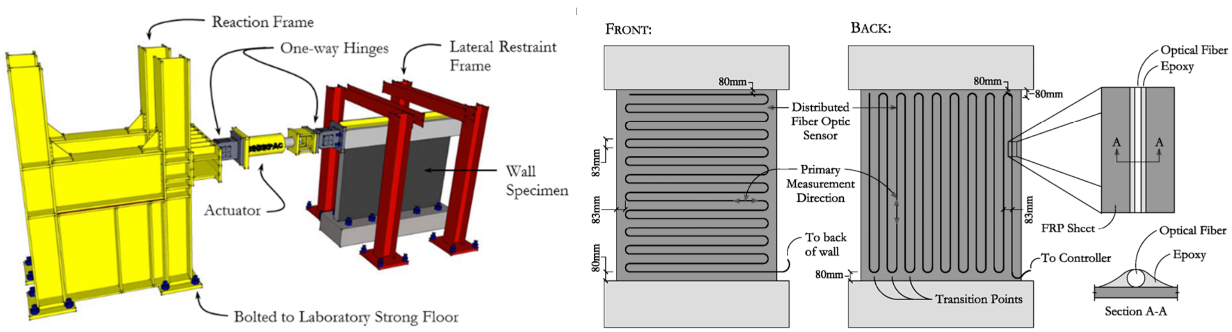

Figure 3.2 Test setup (left) and distributed fiber optic system layout (right)

3.3 Cyclic Behavior and Failure Modes

One of the primary goals in the implementation of the OFDR system is to capture the detailed failure mechanisms of the concrete and the FRP as well as their contribution to the seismic resistance of the shear wall. This information can be utilized in developing a better understanding of the behaviour of RC shear walls retrofitted with FRP sheets. Current design standards for the use of externally bonded FRP sheets [12,13] separate five different failure modes prominent in the behavior of RC element strengthened using FRP sheets. Those failure modes include: (1) crushing of the concrete in compression prior to yielding of vertical steel reinforcement, (2) yielding of reinforcing steel and rupture of the FRP laminate in tension, (3) yielding of the steel in tension followed by concrete crushing in compression, (4) shear/tension delamination of the concrete cover, (5) debonding of the FRP from the concrete substrate (FRP debonding). Failure modes (4) and (5) occur when the FRP laminate separates or debonds from the concrete substrate. In such cases, debonding of the FRP laminate occurs before the material reaches its ultimate tensile strength, thus reducing the capacity of the retrofitted member. To account for debonding, and avoid strength overestimation, modern design standards limit the strain in the FRP to the strain at which debonding is assumed to occur. Eq. 3.1 gives the limit on the strain for flexural FRP reinforcement (ε_{fd}) in the ACI design standard [13]:

$$\varepsilon_{fd} = 0.41\sqrt{\frac{f_c^{'}}{nE_f t_f}} \leq 0.9\varepsilon_{fu} \tag{3.1}$$

where n is the number of vertically oriented FRP plies, E_f is the tensile modulus of the FRP, t_f is the nominal thickness of one ply of FRP reinforcement, and ε_{fu} is the rupture strain of the FRP reinforcement. For a single sheet of vertical

FRP on each side of the wall, the limiting debonding strain value according to Eq. 3.1 is 0.0081. Alternatively, the CSA design standard [12] limits the effective strain in the FRP to 0.007 in vertical FRP laminate, which agrees with the assumption made by the ACI design standard [13]. To determine the limiting strain (ε_{fe}) for the horizontal FRP reinforcement, the ACI design standard [13] provides the following expression:

$$\varepsilon_{fe} = \kappa_v \varepsilon_{fu} \leq 0.004 \tag{3.2}$$

where (κ_v) is a bond reduction coefficient that depends on the concrete strength, the type of wrapping scheme utilized and the stiffness of the laminate. For the walls in this study, the bond coefficient (κ_v) is 0.133, resulting in a limiting debonding strain of 0.0023. In the CSA design standard [12], the effective strain in the horizontal FRP is limited to 0.004, which is higher than the limit from the ACI standard [13] because the CSA standard does not take into consideration the number of horizontal layers applied. Using the OFDR to capture the strain distribution in the FRP sheet will allow for comparison with the limiting debonding strains from current code provisions. Results will also assist in identifying the governing mode of failure and quantify the contribution from the FRP sheet to the seismic performance of the wall. This information will ultimately contribute to improving current design practices and guidelines for the application of FRP sheets in seismic repair and strengthening applications.

4.0 EXPERIMENTAL RESULTS

Results from the experiment indicate that the OFDR performs well in capturing the strain distribution in the FRP along the length of the fiber. Fig. 4.1 shows a typical output from the OFDR over the entire length of the fiber at the cracking, yield and ultimate load. The transition points identified in Fig. 4.1 are regions over which the fiber changes direction. Results show that the vertical strain in the FRP is approximately two times larger than the horizontal strain. The vertical FRP experiences the highest strain along the base of the wall, close to the edges of the wall where the FRP is subject to the highest tensile stresses. The stress in the vertical FRP decreases from the location of the highest stress at the edge of the wall towards neutral axis. The highest strains in the horizontal FRP occur in the center of the wall, and follow and approximately parabolic distribution over the length of the wall.

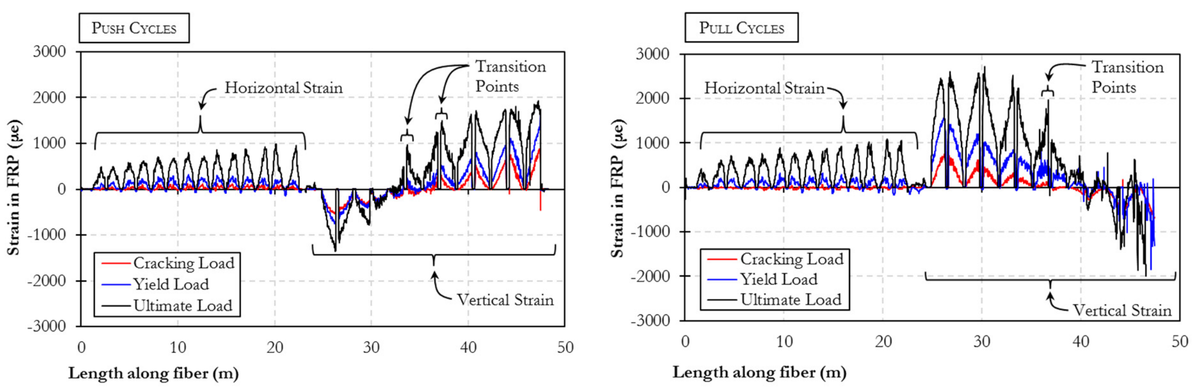

Figure 4.1 Typical output from OFDR sensor system

Using the output from the OFDR, strain profiles in the vertical and horizontal FRP at important locations over the face of the wall can be compared with the strains in the steel reinforcement measured using conventional strain gauges. For the vertical FRP reinforcement, the critical location of interest is along the base of the wall, where the maximum stress develops in the FRP. The strain profile in Fig. 4.2 shows that the up to the yield load, the strain distribution in the FRP and reinforcing steel remains approximately linear, and the neutral axis lies at approximately 2/3 of the walls length. The strain profile at the ultimate load is shown in Fig. 4.2. At the ultimate load, significant concrete crushing at the base of the wall prevents the vertical FRP from reaching its ultimate tensile strength. The vertical FRP reaches a maximum strain of approximately 0.0024, which is significantly less than the limiting debonding strains of 0.007 and 0.0081 recommended by the design standards [12,13]. This information is important for design of FRP retrofitting system as significant concrete crushing and steel yielding before the FRP approaches the debonding strain limits the ability of the FRP to achieve its full ultimate strength. This demonstrates the importance of taking all five failure modes described in section 3.3 into consideration during the design process and ensuring the strength of the wall is not overestimated.

Fig. 4.3 compares the strain distributions in the horizontal FRP and the uppermost horizontal steel stirrup at the cracking and ultimate loads. Results show that at the cracking load, the majority of the horizontal stress is carried by the steel stirrups. However, at the ultimate load carrying capacity, the shear stress is carried approximately equally by the steel stirrups and horizontal FRP. The variable distribution in the horizontal FRP strain at the cracking load indicate locations of initial cracks in the concrete. At the location of these cracks, the steel and FRP are responsible for transferring the shear stress across the crack. At areas in between cracks, concrete, steel, and FRP all contribute together to resisting the shear stresses in the wall. At the ultimate load, significant cracking in the concrete results in higher horizontal strains in the FRP. Because the FRP is responsible for transferring the shear stresses across many cracks in the concrete, this creates a more even stress distribution, with smaller local minima and maxima. The ultimate strain in the horizontal FRP sheets (0.0012) is significantly less than the limiting debonding strains recommended by the design standards [12,13] because of the concrete compression failure in the toes of the wall and longitudinal steel yielding prior to the horizontal FRP approaching the limiting debonding strain values.

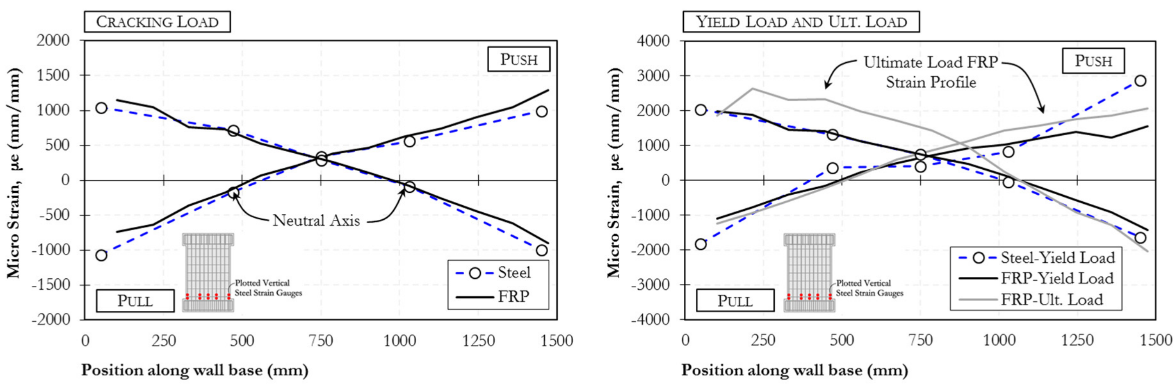

Figure 4.2 Vertical steel and FRP strain profiles at cracking load (left) and yield/ultimate load (right)

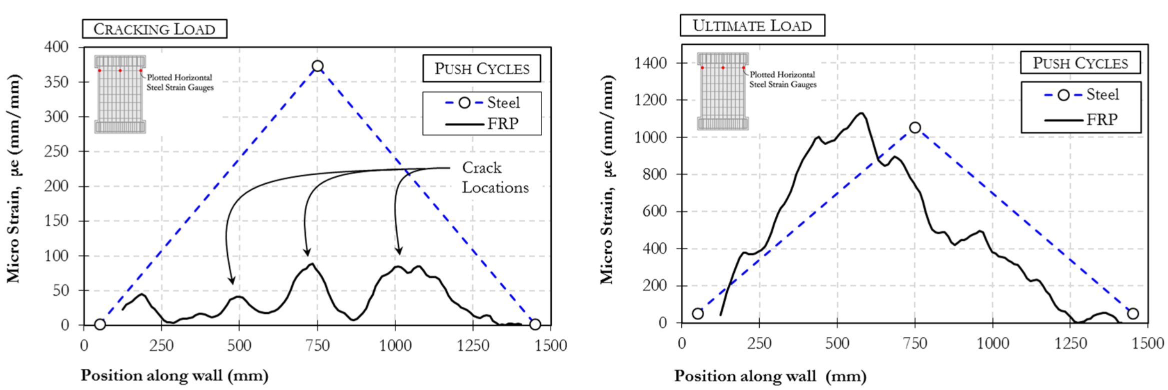

Figure 4.3 Horizontal steel and FRP strain profiles at cracking load (left) and yield/ultimate load (right)

In addition to the strain profiles in the FRP at different load stages, a complete two-dimensional spatial distribution of the strain in the FRP can be constructed using the x and y coordinates and the magnitude (μ-strain) at each measurement point along the fibers length. Given that there is a total fiber length of approximately 25m on each side of the wall, and a measurement point every 10mm, this forms a very high-resolution spatial distribution of the strain in the FRP. Fig. 4.4 shows the 2D spatial strain distribution for retraction (pull) cycles at the cracking load, yield load, ultimate load and at failure of the wall specimen. Results confirm previous observations from the strain distribution analysis that the maximum strains in the FRP sheet occur closest to the base of the wall and vertical stresses are concentrated in the at the edges of the wall. Horizontal stresses are shown to be the highest close to the center of the wall. Areas of localized strain in the horizontal distribution once again represent crack locations, where the FRP is responsible for transferring shear stresses across diagonal cracks in the concrete. This detailed analysis of the strain distribution in the FRP and the ability of the OFDR to capture local strain distributions in 2D over the entire face of the wall is something that cannot be feasibly achieved using conventional strain sensors because of the vast number of sensors required, extended installation time, and cost of the instrumentation. Use of the OFDR system is shown to be useful in understanding the contribution from the FRP to the lateral load resistance of the wall. Results also allowed for comparison between maximum strains in the FRP sheets and those used in design, something that cannot be evaluated in such detail using conventional strain measurement systems.

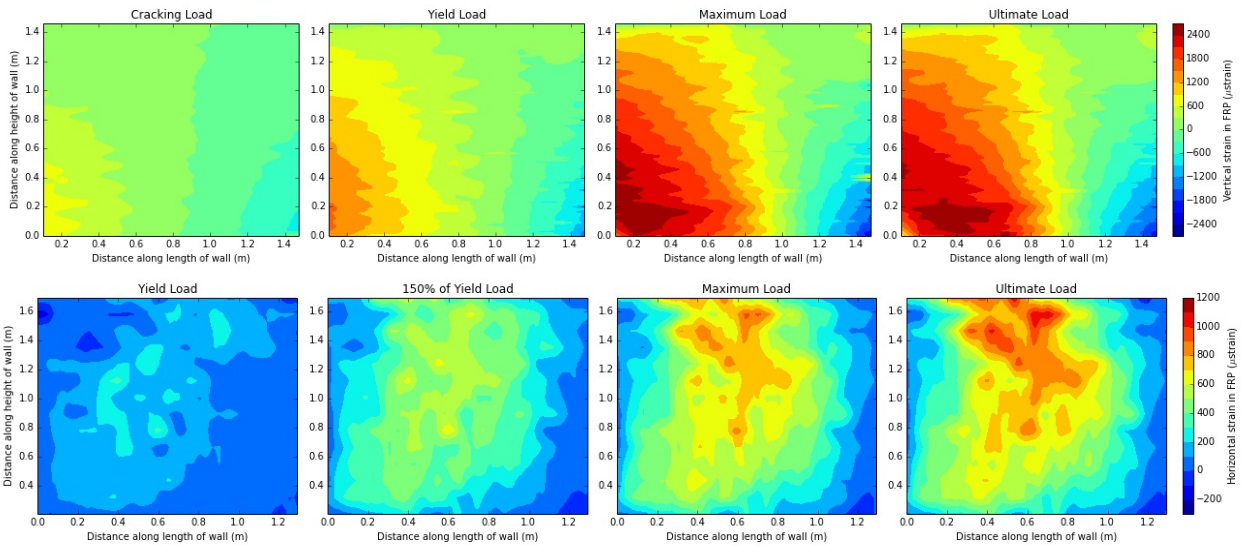

Figure 4.4 2D spatial strain distribution in the vertical FRP (top row) and horizontal FRP (bottom row)

5. OTHER APPLICATIONS

In this study, the OFDR is utilized in a controlled laboratory environment to measure the 2D strain distribution over the face of an FRP-strengthened RC shear wall. The OFDR is shown to be capable of accurately measuring the strain in the FRP at the cracking load, yield load and during the post-peak response of the shear wall. However, the applications for this technology in civil engineering projects is not strictly limited to laboratory experiments and shows great potential for use in other areas of civil engineering, particularly in field applications. The ability to measure strain and temperature at a large number of locations without a priori selection of measurement locations along the length of a single fiber makes the technology ideal for applications in structural health monitoring [14]. In addition, this OFDR sensing system has the added capability of distributed vibration sensing [15], which is essential for dynamic and internal crack identification. The sensors' high resistance to harsh environmental conditions and the low investment costs required for their integration into new or existing infrastructure make them a very attractive and unique alternative to other conventional techniques for long-term monitoring of civil infrastructure. For example, the system lends itself well to applications in structures that require measurements over very large distances (km) such as bridges, dams and pipelines [14]. Conventionally, qualified engineers trained in visual inspection evaluate and inspect the condition of these types of structures at specific time intervals over the service life of the structure. This process can be inaccurate due to human error but is also limited by the time between inspections, during which significant damage could occur to the structure. This problem can be eliminated through the use of the DFOS system, which would allow for continuous monitoring of a structure throughout its service life, and allow for repairs to be conducted at the earliest time and in the most cost-effective manner, thereby minimizing repair and maintenance costs and enhancing the safety and performance of the monitored structure. The DFOS system also has the unique ability to be integrated into the construction of a structure, allowing engineers to monitor response and performance indicators previously not possible, for example, the long-term losses in a bridge prestressing strand. Ultimately, fiber-optic sensors have the potential to increase inspection performance and safety of civil engineering infrastructure.

6. CONCLUSION

A truly distributed fiber optic sensing system based on OFDR using a polarization maintaining fiber is shown to provide very high spatial resolution (mm) and high sensitivity to strain. In doing so, this system offers significant advantages over other conventional systems and other fiber-optic strain measurement systems such as fiber Bragg grating, in that the OFDR based fiber optic sensing system allows measurement to be captured at any point along the length of a single fiber. The OFDR system does not require a priori knowledge of specific measurement locations, which allows unprecedented flexibility and high resolution in strain measurement. The DFOS offers continuous measurement at small increments (10mm) along a single fiber, which can be easily installed, providing cost savings in reducing the number of sensors required and time savings during sensor installation. In this study, the DFOS is implemented in an experimental program on the seismic retrofit of RC shear walls. The shear wall specimen is retrofitted using externally bonded FRP in an attempt to improve its seismic performance. The DFOS is used to measure the strain in the externally bonded FRP sheet, something that would previously have required a large number of sensors. The DFOS is shown to be able to capture the two-dimensional strain distribution over the entire face of the shear wall. This information assists in determining the failure particular failure mode of the shear wall and to assess the contribution from the FRP to the overall seismic resistance to the wall. Ultimately, the DFOS is shown to be extremely successful in a controlled laboratory environment, and shows great potential for use in field applications, including structural health monitoring of large civil engineering structures.

ACKNOWLEDGEMENTS

The authors would like to acknowledge funding provided by the Natural Sciences and Engineering Research Council as well as material and technical contributions from Fyfe Co. and Fibrwrap construction.

REFERENCES

1. Bao, X., Chen, L. (2012). Recent Progress in distributed fiber optic sensors. *Sensors*. **12**, 8447-8486.
2. Li, W., Chen, L., Bao, X. (2013). Compensation of the temperature and strain coefficient due to position dependent birefringence of PMF in OFDR. *Optics Communications*. **311**, 26–32.
3. Bao, X., Webb, D. J., Jackson, D. A. (1994). Combined distributed temperature and strain sensor based on Brillouin loss in an optical fiber. *Optics Letters.* **19:2**, 141-143.
4. Alahbabi, M. N., Cho, Y. T., and Newson, T. P. (2005). Simultaneous temperature and strain measurement with combined spontaneous Raman and Brillouin scattering. *Optics Letters.* **30:11**, 1276-78.
5. Bolognini, G., and Soto, M. A. (2010). Optical pulse coding in hybrid distributed sensing based on Raman and Brillouin scattering employing Fabry-Pérot lasers. *Optics Expresss.* **18:8**, 8459-8465.
6. Xu, M. G., Archambault, J., Reekie, L., and Dakin, J. P. (1994). Discrimination between strain and temperature effects using dual-wavelength fiber grating sensors. *Electronic Letters*. **30:13**, 1085-91.
7. American Concrete Institute (ACI) 318 (1968). Building Requirements for Structural Concrete. Detroit, Michigan, USA. American Concrete Institute.
8. Canadian Standards Association (CSA) (1977). Code for the Design of Concrete Structures for Buildings. *CAN3-A23.3-M77.* Rexdale, Ontario, Canada: Canadian Standards Association.
9. Cruz-Noguez, C. et al. (2014). Seismic Behaviour of RC Shear Walls Strengthened for In-Plane Bending Using Externally Bonded FRP Sheets. *Journal of Composites for Construction.* **19:1**.
10. Woods, J. (2014). Seismic Retrofit of Deficient RC Shear Walls using Fibre-reinforced Polymer Sheets: Experimental Study and Anchor Design. *Master's Thesis*. Carleton University. Ottawa, Canada.
11. Maaskant, R. et al. (1997). Fiber-optic Bragg grating sensors for bridge monitoring. *Cement and Concrete Composites.* **19:1**, 21-33.
12. Canadian Standards Association (CSA) (2002). Design and construction of building components with fibre-reinforced polymers." CAN/CSA S806-02. Rexdale, Ontario, Canada: Canadian Standards Association.
13. American Concrete Institute (ACI) 440.2 (2008). Guide for the Design and Construction of Externally Bonded FRP Systems for Strengthening Concrete Sturctures. Detroit, Michigan, USA.: American Concrete Institute.
14. Bao, X. and Chen, L. (2011). Recent progress in Brillouin scattering based fiber sensors. *Sensors.* **11:4**.
15. Zhou, D., Qin, Z., Li, W., Chen, L., and Bao, X. (2012). Distributed vibration sensing with time-resolved optical frequency-domain reflectometry. *Optics Express*. **20:12**, 13138-13145.